

Oceanographic preferences of Atlantic bluefin tuna, *Thunnus thynnus*, on their Gulf of Mexico breeding grounds

Steven L. H. Teo · Andre M. Boustany ·
Barbara A. Block

Received: 26 November 2006 / Accepted: 21 June 2007 / Published online: 18 July 2007
© Springer-Verlag 2007

Abstract Electronic tagging and remotely sensed oceanographic data were used to determine the oceanographic habitat use and preferences of Atlantic bluefin tuna (*Thunnus thynnus* L.) exhibiting behaviors associated with breeding in the Gulf of Mexico (GOM). Oceanographic habitats used by 28 Atlantic bluefin tuna exhibiting breeding behavior (259 days) were compared with available habitats in the GOM, using Monte Carlo tests and discrete choice models. Habitat utilization and preference patterns for ten environmental parameters were quantified: bathymetry, bathymetric gradient, SST, SST gradient, surface chlorophyll concentration, surface chlorophyll gradient, sea surface height anomaly, eddy kinetic energy, surface wind speed, and surface current speed. Atlantic bluefin tuna exhibited breeding behavior in the western GOM and the frontal zone of the Loop Current. Breeding areas used by the bluefin tuna were significantly associated with bathymetry, SST, eddy kinetic energy, surface chlorophyll concentration, and surface wind speed, with SST being the most important parameter. The bluefin tuna exhibited significant preference for areas with continental slope waters (2,800–3,400 m), moderate SSTs (24–25 and 26–27°C), moderate eddy kinetic energy (251–355 cm² s⁻²), low surface chlorophyll concentrations (0.10–0.16 mg m⁻³), and moderate wind speeds (6–7 and 9–9.5 m s⁻¹). A resource selection function of the bluefin tuna in the GOM was estimated using a discrete choice model and was found

to be highly sensitive to SST. These habitat utilization and preference patterns exhibited by breeding bluefin tuna can be used to develop habitat models and estimate the probable breeding areas of bluefin tuna in a dynamic environment.

Introduction

In marine fishes, the location and timing of spawning determine the environmental conditions experienced by spawning and larval fishes, which in turn affect their reproductive success (Bakun 1996; Chambers 1997). The location and timing of spawning (i.e., habitat use during spawning) are a function of specific environmental preferences and available environmental conditions (Manly et al. 2002; Matthiopoulos 2003). It is therefore important to quantify the environmental preferences of the spawning fish because it will help determine essential spawning habitat, predict the possible effects of habitat and climate change, and test hypotheses about ecological processes (Arthur et al. 1996; Laidre and Heide-Jorgensen 2005; Rice 2005). The use of electronic tags has improved our understanding of the habitat use and preferences of several pelagic species, by integrating biological and physical data from electronic tags with ocean observation data sets from satellites, buoys, and numerical models (e.g., Block et al. 2002, 2005; Polovina et al. 2004; Baumgartner and Mate 2005). However, our understanding of the environmental preferences of spawning pelagic fish remains poor (Schaefer 2001; Teo et al. 2007).

In this study, we integrate electronic tag data with remotely sensed oceanographic datasets to determine the oceanographic habitats in the Gulf of Mexico (GOM) used by breeding Atlantic bluefin tuna (*Thunnus thynnus*). The

Communicated by J.P. Grassle.

S. L. H. Teo (✉) · A. M. Boustany · B. A. Block
Tuna Research and Conservation Center,
Hopkins Marine Station, Stanford University,
120 Oceanview Boulevard,
Pacific Grove, CA 93950, USA
e-mail: lteo@ucdavis.edu

western Atlantic stock of Atlantic bluefin tuna is known to spawn primarily in the GOM from April to June (Magnuson et al. 1994; Mather et al. 1995; Schaefer 2001; Block et al. 2005). Using electronic tags, we have shown that western Atlantic bluefin tuna exhibit three distinct phases (entry, breeding, and exit phases) of movement paths, diving behavior and thermal biology, on their breeding grounds in the GOM (Teo et al. 2007). As the bluefin tuna enter and exit the GOM, the fish dive to significantly deeper daily maximum depths (>500 m), and exhibit directed movement paths to and from areas where the fish exhibit breeding-specific behaviors. In the breeding phase, the fish exhibit significantly shallower daily maximum depths, perform shallow oscillatory dives, and have movement paths that are significantly more residential and sinuous (Teo et al. 2007). In addition, the tags also recorded the highest water and body temperatures during the night of the breeding phase. Based on these parameters, we hypothesized the tags were recording courtship and/or spawning behaviors, and use the tag data to identify the locations and times of the breeding phase. Subsequently, we combine this information with remotely sensed oceanographic data sets to quantify the habitat usage and the available habitat during the breeding phase.

One of our aims is to determine the oceanographic preferences of breeding western Atlantic bluefin tuna but it is difficult to measure habitat preferences directly (Johnson 1980; Arthur et al. 1996; Manly et al. 2002). It is more tractable to first quantify habitat use and the available habitat, and to subsequently use resource selection models and indices to quantify habitat preferences (Johnson 1980; Arthur et al. 1996; Manly et al. 2002). We first use Chesson's preference index (Chesson 1978, 1983) coupled with Monte Carlo methods (Baumgartner and Mate 2005) to visualize and estimate the univariate habitat preferences of the bluefin tuna. Subsequently, we use a discrete choice model to estimate a resource selection function (RSF) (Cooper and Millsbaugh 1999; McDonald et al. 2006).

The GOM has distinct oceanographic characteristics, which can be conveniently divided into eastern and western GOM. The eastern GOM is dominated by the Loop Current, which flows north through the Yucatan Straits and makes an anti-cyclonic turn before exiting through the Florida Straits. The Loop Current has a flow that varies from 23 to 35 Sv (Hamilton et al. 2005) and meanders as it approaches the Florida Straits. These meanders create alternating zones of positive and negative vorticity, which in turn generate alternating zones of enhanced production and retention, respectively (Bakun 1996). Richards et al. (1989) observed that Atlantic bluefin tuna larvae were associated with the Loop Current frontal zone. This led Bakun (1996) to hypothesize that Atlantic bluefin tuna may be preferentially using the Loop Current frontal zone for

spawning because of the alternating zones of positive and negative vorticity. However, other larval surveys showed that the majority of bluefin tuna larvae were found in the western GOM (Nishida et al. 1998). One of the key oceanographic features in the western GOM is cyclonic and anti-cyclonic mesoscale eddies generated by or pinched off from the Loop Current, which travel from east to west (Dietrich and Lin 1994). The cyclonic eddies in the western GOM are associated with enhanced primary and secondary production (Gasca 1999, 2003; Wormuth et al. 2000; Gasca et al. 2001; Suarez-Morales et al. 2002).

The spawning stock of Atlantic bluefin tuna in the western Atlantic has declined by >90% over the past 30 years (ICCAT 2005). One of the management and conservation issues facing Atlantic bluefin tuna is the need for protection on their GOM spawning grounds. The International Commission for the Conservation of Atlantic Tunas (ICCAT, <http://www.iccat.es>), which manages Atlantic bluefin tuna, recognizes the importance of protecting spawning grounds and has prohibited directed fishing for bluefin tuna in the GOM since 1982 (Magnuson et al. 1994). However, there is current concern about the incidental bycatch of mature bluefin tuna by the U.S. yellowfin tuna longline fishery in the GOM (Block et al. 2005). The National Oceanic and Atmospheric Administration (NOAA) has instituted fishery observer programs to document the bycatch and subsequently enacted regulations to reduce the bycatch (O'Brien et al. 2004). Nevertheless, the large number of longline hooks in the breeding area is still resulting in high mortality rates (Block et al. 2005). By understanding the habitat use and oceanographic preferences of bluefin tuna breeding in the GOM, we can identify essential breeding habitat. In doing so, this will help NOAA scientists to model the breeding habitat selected by the fish and reduce bluefin bycatch in the GOM.

Materials and methods

Electronic tag data

From 1996 to 2004, 772 Atlantic bluefin tuna (*T. thynnus* L.) were tagged with either implantable archival tags (499) or popup satellite archival tags (PAT, 273) in North Carolina, Massachusetts, and the GOM (Block et al. 2005). The experimental procedures have previously been described in detail (Block et al. 1998a, b, 2001; Teo et al. 2007). Five models of archival tags (NMT v1.1 and v1.2, Northwest Marine Technology, USA; Mk7 v1 and v2, Wildlife Computers, USA; and the LTD 2310, Lotek Wireless, Canada) and four versions of PAT tags (Wildlife Computers, USA; hardware versions 1–4) were deployed. These electronic tags recorded depth, water temperature,

and light level data. In addition, the archival tags also recorded the peritoneal temperature of the fish.

Bluefin tuna geolocations were estimated from light level and sea surface temperature (SST) data recorded by the tags (see Teo et al. 2004 for a detailed description). For PAT and Mk7 archival tags, a proprietary software package from the tag manufacturer (WC-GPE Suite v1.1.5.0, Wildlife Computers) was used to correct for light attenuation and to estimate longitudes from the light level data. The LTD 2310 and NMT archival tags had onboard software that processed the light level and pressure data, corrected for light attenuation, and logged the estimated longitude into the ‘day log’ (Ekstrom 2004). Sea surface temperatures from the tags were combined with corresponding light level longitude estimates to obtain daily latitude estimates (Teo et al. 2007). For a given day, the latitude at which tag-recorded SSTs best matched corresponding remotely sensed SSTs along the light level longitude estimate was considered the latitude estimate for the day (Teo et al. 2004).

Geolocations estimated from light and SST data were combined with the corresponding tagging, popup endpoint and/or reported recapture locations to generate a dataset with 13,372 geositions (Block et al. 2005). Based on this dataset, 36 bluefin tuna were located within the GOM and 28 of these fish returned enough electronic tag data from the GOM for further analysis (see Table 1 in Teo et al. 2007).

The locations and timing of each bluefin tuna’s breeding phase were identified from their electronic tag data using the method described in Teo et al. (2007). The geolocation, depth, ambient, and body temperature data from the GOM were extracted and used to analyze their movement paths, diving behavior, and thermal biology. For each fish, we determined the daily maximum depths during its period in the GOM and filtered the maximum depths using a 3-day median boxcar filter. The maximum depth was used because it was the most common depth data collected and returned by both archival and PAT tags. The overall mean of the filtered maximum depths was calculated, and the central portion of the period in the GOM that was shallower than the mean was considered the breeding phase. Subsequently, the diving behavior from the three phases was visually examined to ensure that the algorithm performed adequately. We extracted the movement paths of the fish and used the identified breeding phase locations and dates ($n = 259$ days) to determine their habitat utilization and preference patterns.

Oceanographic data

We determined habitat use and preference patterns for ten oceanographic parameters—bathymetry, bathymetric

gradient, SST, SST gradient, surface chlorophyll concentration, surface chlorophyll gradient, sea surface height anomaly (SSHA), eddy kinetic energy, surface wind speed, and surface current speed. A 2’ by 2’ global topographic dataset derived from ship soundings and satellite altimetry data (Smith and Sandwell 1997) were downloaded from the Scripps Institution of Oceanography (ftp://topex.ucsd.edu/marine_topo/). Two small islands at approximately 25.53°N, 90.42°W were found to be spurious and were removed from the dataset. Bathymetry values for the deleted area were subsequently filled by interpolating from neighbouring pixels. Bathymetric gradients were calculated by performing a two-dimensional convolution on the GOM bathymetry grid, with a 3 × 3 pixel Sobel filter (Russ 2002; Baumgartner and Mate 2005). The Sobel filter is used in image processing to determine the magnitude and direction of the gradients and edges in an image (Russ 2002). The scalar gradient magnitude, G , of each pixel was calculated by,

$$G = \sqrt{G_x^2 + G_y^2} \quad (1)$$

where G_x and G_y were the zonal and meridional bathymetric gradients of each pixel, respectively.

We obtained gridded SSTs from the Advanced Very High Resolution Radiometer (AVHRR) sensors (Pathfinder SST, <http://www.podaac.jpl.nasa.gov>). The SSTs for the GOM from 1999 to 2005 were extracted. The data grids consisted of 8-day and monthly averaged SSTs on a nominal 4-km equal angle grid. We preferentially used 8-day grids but the monthly grid was used if the cloud cover at the fish’s location was >50%. Cloud cover was calculated from the spatial kernel average of a location (see Analysis subsection for a detailed explanation of spatial kernel averaging). The SST gradients were calculated in the same manner as bathymetry gradients.

Surface chlorophyll concentration data from the Sea-viewing Wide Field-of-view Sensor (SeaWiFS) and the Moderate Resolution Imaging Spectroradiometer (MODIS/Aqua) were downloaded (<http://www.oceans.gsfc.nasa.gov>). From 1999 to 2002, we used the data from SeaWiFS. From 2003 to 2005, we used merged data from both SeaWiFS and MODIS/Aqua, which reduced the cloud cover in the 8-day data by about 20%. The downloaded data consisted of 8-day and monthly averaged chlorophyll concentration data on a 9-km equal angle grid. Similar to the SST data, the 8-day datasets were used preferentially but the monthly grid was used if the cloud cover for the 8-day grid at the fish’s location exceeded 50%. Chlorophyll concentration gradients were calculated in the same manner as bathymetry gradients.

We downloaded SSHA and geostrophic velocity anomaly data for the GOM, which were derived from merged satellite altimetry measurements of four satellite altimeters (Jason-1, ENVISAT/ERS, Geosat Follow-On and Topex/Poseidon interlaced) (AVISO, <http://www.avisioceanobs.com>). The SSHA and geostrophic velocity anomaly data extended from 1993 to 2005, with data assimilated every 7 days on a $1/3^\circ$ Mercator grid. Geostrophic velocity anomalies during the breeding season (March–June) were used to calculate the eddy kinetic energy (EKE) in the GOM. Eddy kinetic energy is a commonly used measure of the mesoscale variability of the flow in a region and helps to identify regions where mesoscale eddies and current meanders are relatively common (e.g., Stammer 1998; Ducet et al. 2000; Pascual et al. 2006; Waugh et al. 2006). The EKE (per unit mass) was calculated by

$$\text{EKE} = \frac{1}{2} (u'^2 + v'^2) \quad (2)$$

where u' and v' were the zonal and meridional velocity anomalies, averaged over March to June from 1993 to 2005.

We downloaded ocean surface wind speed data from the ERS-1/2 and QuikSCAT satellite scatterometers (<http://www.oceanwatch.pfeg.noaa.gov>). For 1999, we used the wind speed data from the ERS-1/2 satellites, which were on a 1.0° equal angle grid. From 2000 to 2005, we used the wind speed data from the QuikSCAT satellite, which were on a 0.5° equal angle grid. All the surface wind speed data consisted of 8-day averaged grids.

We obtained surface current velocity data, which were derived from merged satellite altimeter and scatterometer data from Collecte Localisation Satellites (CLS, <http://www.cls.fr>). Surface currents were calculated by adding the geostrophic flow derived from the absolute dynamic topography from four satellite altimeters (Jason-1, ENVISAT/ERS, Geosat Follow-On and Topex/Poseidon interlaced) to the Ekman component derived from the ocean surface wind velocity data (Gaspar et al. 2006; Pascual et al. 2006). We obtained surface current velocity data for the GOM every 7 days on a 0.25° grid from 1999 to 2005 during the breeding months.

Analysis

Oceanographic habitat use patterns of breeding phase Atlantic bluefin tuna were quantified from spatial kernel samples of oceanographic data at the location and date of each breeding phase geolocation estimate. A spatial kernel sample is a spatially weighted average of the data using a specified spatially explicit function. We used spatial kernel

sampling in order to account for the error distribution associated with each geolocation estimate. For archival tags, the error distributions of the geolocation estimates were approximated by bivariate Gaussian distributions with standard deviations (σ) of 0.78° and 0.90° in the zonal and meridional directions, respectively (Teo et al. 2004). For PAT tags, the error distributions of the geolocation estimates were approximated by bivariate Gaussian distributions with σ s of 1.30° and 1.89° in the zonal and meridional directions, respectively (Teo et al. 2004).

Separate $2\text{-}\sigma$ spatial kernels for archival and PAT tags were created from their respective error distributions, which would encompass the 95% confidence intervals of the geolocation estimates. The spatial kernels can be visualized as three-dimensional normal distributions, with the x and y directions corresponding to the zonal and meridional coordinates, and the height of the kernel corresponding to the probability that the fish was at that location. For each geolocation estimate, an oceanographic data grid was obtained for the corresponding date. The spatial kernel was placed over the data grid, with the center of the spatial kernel over the pixel corresponding to the geolocation estimate. If the geolocation estimate was from an archival tag, the spatial kernel based on the error distribution of an archival tag was used, and similarly for a PAT tag. A weighted average of the oceanographic data was then calculated using weights corresponding to the height of the spatial kernel over each pixel. This weighted average was considered as the oceanographic habitat used by the fish for that day. Bathymetric gradient, SST gradient, EKE, chlorophyll concentration, chlorophyll gradient, and surface current speed were log-transformed to improve the linearity of the data.

Oceanographic habitats available to the bluefin tuna were determined from spatial kernel samples of oceanographic data at the locations from null model movement paths, which were generated by Monte Carlo methods (Baumgartner and Mate 2005). For each fish, we randomly generated 10,000 null model movement paths with the initial position of the generated paths being identical to the initial location of the observed paths. The initial position for fish tagged in the GOM would be their tagging location, whereas the initial position for fish entering the GOM from the Atlantic Ocean would be their first geolocation west of 80°W . Segment distances (distance between geolocations) were identical to the observed track but travel direction of each segment was randomly generated from a uniform distribution. The generated positions were not allowed to occur on land or exit the GOM. At each generated location, we made a spatial kernel sample of the oceanographic habitat using the same method as the observed tracks.

Using null model movement paths and spatial kernel sampling to calculate available habitat has two main advantages. The habitat available to an animal at time $t + 1$

is autocorrelated with the location of the animal at time t and the distance traveled by the animal between times t and $t + 1$. If the available habitat is calculated from a fixed area larger than that traveled in a single time step, the estimated habitat preferences of the animal will likely be inaccurate (Manly et al. 2002). Since the null model movement paths were generated using the movement characteristics of each individual animal, the magnitude of the autocorrelation for each location and time step in the generated paths were identical to that of the observed paths. This would therefore ‘side-step the problem’ of spatiotemporal autocorrelation in the analysis (Matthiopoulos et al. 2004). In addition, the uncertainty in the geolocation estimates is explicitly accounted for in both the observed habitat use and the available habitat data with the spatial kernel samples. It is important to note that the spatial kernel samples of the environment are statistical representations of the environment experienced by the fish rather than the actual environment. As with any statistical representation, there will be errors associated with it, and the estimated RSF will therefore be approximate. However, this source of error will likely be small compared with the errors inherent in the remote-sensing data.

We used Chesson’s preference index (Chesson 1978, 1983) to visualize and estimate the univariate habitat preference of the fish. The Chesson’s preference index is commonly used to quantify the resource preference (habitat and/or food) of an individual or a group of animals (Manly et al. 2002). The Chesson’s preference index of the i th habitat type, α_i , is calculated by,

$$\alpha_i = \frac{(o_i/\pi_i)}{\sum_{j=1}^n (o_j/\pi_j)} \quad (3)$$

where o_i is the sample proportion of used units in the i th habitat type, π_i is the sample proportion of available units in the i th habitat type, and n is the total number of habitat types. For each oceanographic parameter, we calculated o_i as the normalized frequency of occurrence in the i th bin of the habitat use distribution and π_i as the normalized frequency of occurrence in the i th bin of the distribution of available habitat (see previous paragraph). We subsequently calculated α_i for each histogram of each oceanographic parameter.

Monte Carlo tests were used to determine the probability that the habitat preferences displayed by the Atlantic bluefin tuna could have occurred by chance (i.e., by moving at random, Baumgartner and Mate 2005). For each oceanographic parameter, we calculated the observed Chesson’s index distribution using the i th bin of the normalized frequency histograms of observed habitat use as o_i and the i th bin of the normalized frequency histograms of

available habitat as π_i . We also calculated 10,000 simulated Chesson’s index distributions from the simulated movement paths. At each bin of the frequency histograms, we counted the number of simulations with Chesson’s index value greater than or equal to the observed value. This number can be thought of as the probability that the observed Chesson’s index at that bin could have occurred by chance. The bins with less than 500 of the simulated runs having Chesson’s index values greater than or equal to the observed values were identified. These bins had <5% chance that the preference shown by the fish could have occurred by chance (i.e., $P < 0.05$).

There were two main problems related to using Monte Carlo tests with Chesson’s indices. Firstly, using the Chesson’s index requires binning continuous variables like SST, which may induce bin width artifacts. We addressed this by varying the bin width by approximately 25% (both bigger and smaller) and found that the habitat preference patterns remained relatively robust. Secondly, we conducted multiple Monte Carlo tests, which may result in false positives. We chose not to make Bonferroni-type corrections to the statistical significance levels because we intended this phase of the analysis to be primarily exploratory. In particular, the Chesson’s index was a useful visualization tool for habitat preferences.

In order to address these problems, we used a discrete choice model to estimate the RSF of the breeding bluefin tuna. Discrete choice models are a large class of models commonly used in econometrics to understand the behaviors and preferences of human subjects (Train 2003). In recent years, discrete choice models have been used to analyze habitat selection by animals and estimate their RSFs (McCracken et al. 1998; Cooper and Millsbaugh 1999; Manly et al. 2002; McDonald et al. 2006). One of the key advantages of using discrete choice models in aquatic environments is that the available habitat is not assumed to be static.

In this study, we used the multinomial logit form of discrete choice model, which is the most common form of discrete choice model (Manly et al. 2002; Train 2003). Bluefin tuna were assumed to select an area for spawning based on the available habitat. Since the bluefin tuna may have used the same area repeatedly for spawning, the habitat choices were assumed to have been made with replacement. McDonald et al. (2006) showed that in this scenario, the conditional probability of area i being selected is

$$p(i) = \frac{\exp(\beta_1 x_{i1} + \beta_2 x_{i2} + \dots + \beta_p x_{ip})}{\sum_{k \in \{U \cup A\}} \exp(\beta_1 x_{k1} + \beta_2 x_{k2} + \dots + \beta_p x_{kp})} \quad (4)$$

where $\beta_1, \beta_2, \dots, \beta_p$ are coefficients to be estimated, x_{ij} is the value of oceanographic parameter j for the i th area, the

set U' is the set of used areas, and A is the set of areas in the Monte Carlo sample of areas from the GOM. The likelihood function for the observed data is simply the product of these probabilities,

$$L(\beta_1, \beta_2, \dots, \beta_p) = \prod_{j=n_1}^{n_u} p(j) \quad (5)$$

where n_1, \dots, n_u were the areas used by the bluefin tuna. Following McDonald et al. (2006) and Manly et al. (2002), the coefficient estimates were obtained using a stratified Cox proportional hazards function. (PROC PHREG, SAS 9.1, SAS Inc.). The resulting RSF, which is the relative probability of bluefin tuna using an area in the GOM, is simply the numerator of Eq. 4. We only included parameters in the RSF that were statistically significant ($P < 0.05$). The habitat used by the breeding bluefin tuna and the habitat available were sampled using the spatial kernel samples. We included the longitude and latitude of the locations to test if the bluefin tuna preferentially used certain areas of the GOM. In addition, quadratic terms of all parameters were included in the model because the Chesson's indices indicated that the bluefin tuna often preferred moderate levels of the oceanographic parameters being tested. However, interaction terms were not included due to the lack of degrees of freedom.

We performed a sensitivity analysis on the RSF to determine the relative importance of the various parameters. Sensitivity was calculated as the percent change in the RSF exponent with a 10% change in parameter values, with respect to the mean parameter values from the spatial kernel samples. Increased sensitivity indicated that the parameter more strongly affected the probability of bluefin tuna using an area.

Results

Breeding phase locations ($n = 259$ days) for the 28 Atlantic bluefin tuna (*T. thynnus*) were primarily located over the lower slopes of the northern GOM (Figs. 1, 2). Locations along the slope waters ranged from the western GOM to the frontal zone of the Loop Current (Fig. 1).

The discrete choice model also indicated, as long as the other parameters in the RSF remained constant, the western GOM would have a higher probability of being used (Table 1). The negative coefficient for longitude indicates that the RSF decreases with increasing longitude (eastwardly). In addition, the negative coefficient for the quadratic term indicates that the RSF with respect to longitude is dome-shaped. Negative coefficients for the quadratic terms indicate that the responses are dome-shaped, whereas

positive coefficients indicate bowl-shaped responses. In contrast to longitude, latitude did not significantly affect the probability of bluefin tuna using an area and was not included in the RSF (Table 1).

The breeding locations of bluefin tuna were significantly associated with depths of 2,800 to 3,400 m ($P < 0.05$, 10,000 Monte Carlo samples, Fig. 2). A large proportion (32.8%) of the breeding locations were in areas between 2,800 and 3,400 m (Fig. 2). The discrete choice model indicated that bathymetry significantly affected the probability of bluefin tuna using an area, with deeper waters being more likely to be used (Table 1). In addition, the bluefin tuna significantly preferred the continental slope areas with moderate bathymetric gradients (11.2 to 22.4 m km⁻¹, $P < 0.05$, 10,000 Monte Carlo samples, Fig. 3). However, bathymetry gradient did not significantly affect the probability of bluefin using an area if other environmental parameters were taken into consideration, and was not included in the RSF (Table 1).

The majority of breeding phase locations (88.8%) were located in areas with SSTs ranging from 24 to 29°C (Fig. 4). The bluefin tuna significantly preferred SSTs in the ranges of 24–25°C and 26–27°C ($P < 0.05$, 10,000 Monte Carlo samples, Fig. 4). In addition, the bluefin tuna experienced significantly different SSTs between months, with the warmest SSTs in June ($P < 0.001$, ANOVA, Table 2). Significant preferences for 24–25°C and 26–27°C were exhibited in April and May, respectively. In June, bluefin tuna predominantly used SSTs between 28 and 29°C but no significant preference was detected in this temperature range (Fig. 4). The discrete choice model also indicated that the bluefin tuna significantly preferred moderately warm SSTs (Table 1). Sensitivity analysis of the RSF indicated that SST was by far the most important oceanographic parameter that significantly affected the probability of bluefin tuna using an area for breeding (Table 1). Most of the breeding phase locations (79.2%) were in areas with SST gradients between 0.013 and 0.025°C km⁻¹ but the fish did not exhibit a significant preference for any SST gradient ($P > 0.05$, 10,000 Monte Carlo samples). The discrete choice model also indicated that SST gradient did not significantly affect the probability of bluefin tuna using an area (Table 1).

The majority of the breeding phase locations (56.4%) occurred in waters with low surface chlorophyll concentrations (0.10–0.16 mg m⁻³), and the bluefin tuna exhibited a significant preference for areas with this range ($P < 0.05$, 10,000 Monte Carlo samples, Fig. 5). In addition, the breeding phase bluefin tuna also significantly preferred areas with low chlorophyll gradients (6.3×10^{-4} to 3.2×10^{-3} mg m⁻³ km⁻¹, $P < 0.05$, 10,000 Monte Carlo samples, Fig. 6). This was corroborated by the discrete choice model, which showed that surface chlorophyll and

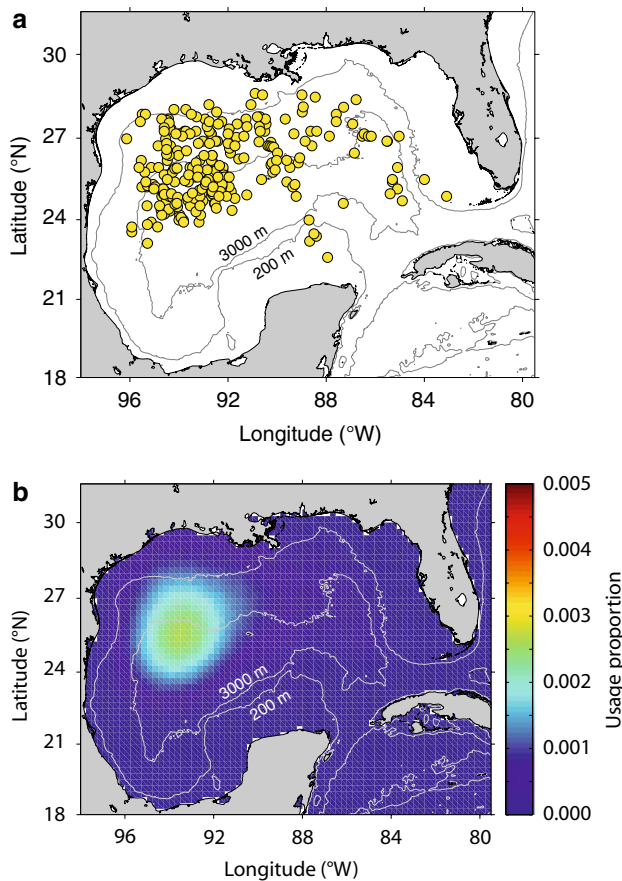


Fig. 1 *Thunnus thynnus*. **a** Geolocations (yellow circles, $n = 259$) of 28 breeding phase Atlantic bluefin tuna. Geolocations were determined from light and sea surface temperature data collected by electronic tags deployed on the fish. 200 and 3,000 m contour lines are shown as gray lines. **b** Observed spatial use of breeding phase Atlantic bluefin tuna ($n = 28$)

chlorophyll gradient significantly affected the habitat use of bluefin tuna (Table 1).

Breeding bluefin tuna used, and significantly preferred areas with moderate eddy kinetic energy, ranging from 251 to 355 $\text{cm}^2 \text{s}^{-2}$ ($P < 0.05$, 10,000 Monte Carlo samples, Fig. 7). A large proportion (48.7%) of the breeding phase locations occurred in these areas (Fig. 7). The discrete choice model analysis indicated that eddy kinetic energy significantly affected the probability of bluefin tuna using an area (Table 1). The main area in the GOM with this moderate level of eddy kinetic energy is the western GOM and to a lesser extent, the edge of the Loop Current (Fig. 7).

In the GOM, this range of eddy kinetic energy is indicative of areas with moderate surface current speeds and the presence of mesoscale eddies. The majority (81.9%) of the breeding phase locations occurred in surface current speeds from 12.6 to 31.6 cm s^{-1} , and the fish significantly preferred these areas with these current speeds ($P < 0.05$, 10,000 Monte Carlo samples, Fig. 8). In addition,

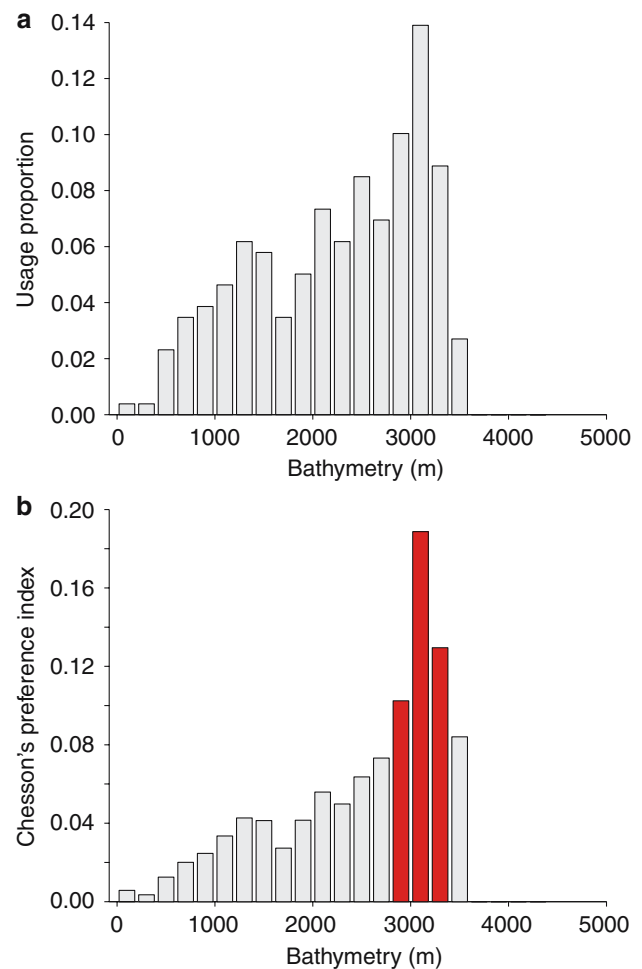


Fig. 2 *Thunnus thynnus*. **a** Observed bathymetric habitat use exhibited by breeding phase Atlantic bluefin tuna ($n = 28$). **b** Bathymetric habitat preference of breeding phase Atlantic bluefin tuna. Red bars indicate bins where fish exhibited significant preference ($P < 0.05$, 10,000 Monte Carlo samples)

the fish exhibited some preference for areas with non-zero SSHA (Fig. 9), which indicates the presence of eddies. However, the preference was not significant ($P > 0.05$, 10,000 Monte Carlo samples, Fig. 9). The discrete choice analysis indicated that surface current and SSHA did not significantly affect the use of an area once the effects of all other parameters were considered (Table 1). However, quadratic term of surface current is marginally insignificant ($P = 0.0544$, Table 1), and may still have a biological effect on habitat use. Although 50.6% of the breeding phase locations had SSHA from -5 to 5 cm , the Chesson's preference indices for these areas were relatively low (Fig. 9), which indicates that the GOM is dominated by areas with SSHA around zero but the fish significantly preferred areas with eddies.

The Atlantic bluefin tuna used and preferred areas with moderate wind speeds, and the majority of the breeding

Table 1 *Thunnus thynnus*. Parameter estimates and sensitivity of resource selection function (RSF) derived from discrete choice model of breeding bluefin tuna habitat preference (to three significant figures)

Parameters	Parameter estimates	Standard error	χ^2	$P > \chi^2$	Sensitivity of RSF (%)
Longitude ^b	-0.0531	0.0137	15.0	0.0001*	13.4
Longitude	-10.2	2.50	16.7	<0.0001*	14.3
Latitude ^b	-0.0862	0.0621	1.93	0.1648	
Latitude	4.84	3.15	2.37	0.1236	
Bathymetry ^b	9.55×10^{-7}	2.91×10^{-7}	10.8	0.001*	0.0779
Bathymetry	0.00311	0.00130	5.72	0.0168*	0.0782
^a Bathymetry gradient ^b	-2.68	1.67	2.59	0.1074	
^a Bathymetry gradient	16.9	9.15	3.42	0.0644	
SST ^b	-0.158	0.0802	3.88	0.049*	3.30
SST	8.57	4.10	4.38	0.0364*	3.45
^a SST gradient ^b	-0.327	1.01	0.105	0.746	
^a SST gradient	-3.13	7.90	0.157	0.6915	
^a Chlorophyll ^b	0.519	0.227	5.23	0.0222*	0.0161
^a Chlorophyll	1.98	0.904	4.81	0.0282*	0.0308
^a Chlorophyll gradient ^b	-0.462	0.139	11.1	0.0009*	0.0144
^a Chlorophyll gradient	-5.20	1.70	9.32	0.0023*	0.0809
SSHA ^b	-0.000261	0.000885	0.0871	0.7679	
SSHA	0.0309	0.0207	2.24	0.1345	
^a Eddy kinetic energy ^b	-0.524	0.217	5.84	0.0157*	0.0163
^a Eddy kinetic energy	6.46	2.59	6.24	0.0125*	0.100
Surface wind ^b	0.117	0.0602	3.76	0.0524	
Surface wind	-1.89	0.791	5.69	0.017*	0.187
^a Surface current ^b	-1.06	0.552	3.70	0.0544	
^a Surface current	-3.22	1.86	2.99	0.0835	

Overall model was highly significant ($\chi^2 = 557.97$, $P < 0.0001$); sensitivity was calculated as percent change in the RSF exponent with a 10% change in mean parameter value

* Parameter was significant ($P < 0.05$) and included in RSF

^a Log-transformed parameter

^b Quadratic term—negative parameter estimate indicates dome-shaped response, and vice versa

phase locations (53.2%) were in such areas ($5\text{--}7 \text{ m s}^{-1}$, Fig. 10). The fish exhibited significant preferences for moderate wind speeds ($6\text{--}7$ and $9\text{--}9.5 \text{ m s}^{-1}$, $P < 0.05$, 10,000 Monte Carlo samples, Fig. 10). The discrete choice model also showed that surface wind speed significantly affected the habitat use of bluefin tuna (Table 1).

Discussion

Electronic tags were used to detect the distinct movement patterns, oscillatory diving behavior, and high body temperatures that characterize Atlantic bluefin tuna (*T. thynnus*) breeding in the GOM (Teo et al. 2007). Diving behavior and horizontal movements were used to estimate the most likely time and location of breeding. Subsequently, the oceanographic habitat use and preferences of

the bluefin tuna were quantified by comparing the oceanographic habitats used, against the habitats available in the GOM.

Previous knowledge of the spatial and temporal spawning distributions of Atlantic bluefin tuna have primarily been obtained from larval surveys and histological examination of reproductive tissues from fishery samples (McGowan and Richards 1989; Schaefer 2001; Block et al. 2005). This study adds to our understanding by using electronic tag data to elucidate the habitat use and preference patterns of breeding bluefin tuna. Of the Atlantic bluefin tuna observed to have spawned in the GOM, the majority of the fish spawned in the western GOM. This result is supported by large-scale larval tuna surveys in the GOM by the RV Shoyo Maru and RV Oregon II, which also found that the majority of larval bluefin tuna are found in the western GOM (Nishida et al. 1998). Bluefin tuna are

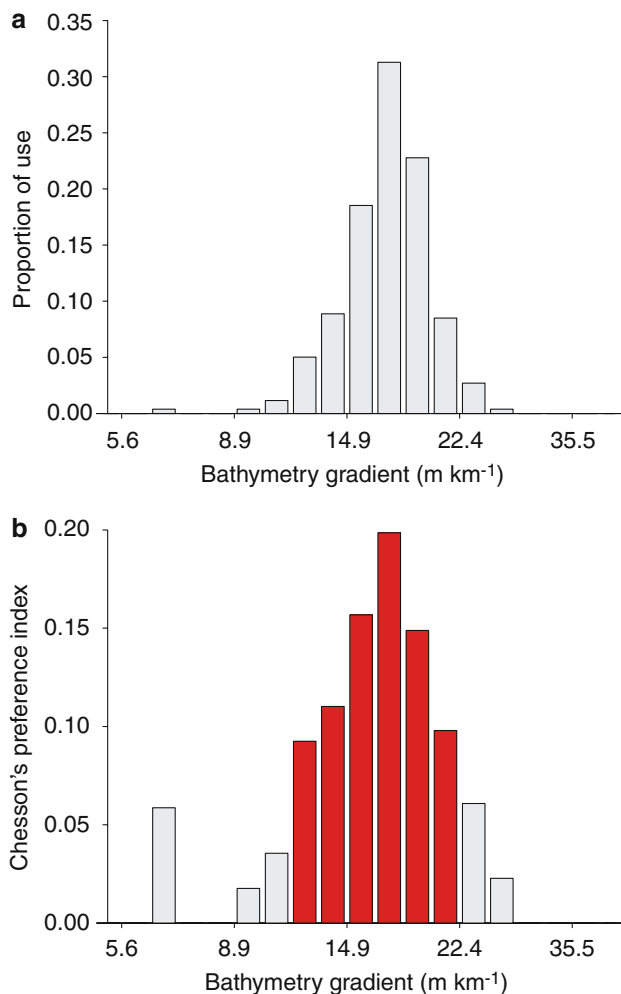


Fig. 3 *Thunnus thynnus*. **a** Observed bathymetric gradient use of breeding phase Atlantic bluefin tuna ($n = 28$). **b** Bathymetric gradient preference of breeding phase Atlantic bluefin tuna. Red bars indicate bins where fish exhibited significant preference ($P < 0.05$, 10,000 Monte Carlo samples)

also using the frontal zone of the Loop Current in the GOM. Geolocation and analysis of breeding behavior indicated that two fish (98–512 in 1999 and A0532 in 2003) exhibited breeding phase behavior near the Loop Current frontal zone (Teo et al. 2007). Detailed larval surveys in the eastern GOM have shown that bluefin tuna larvae are associated with the Loop Current frontal zone (Richards et al. 1989). Therefore, our results from the electronic tagging data of mature bluefin tuna on their breeding grounds are consistent with previous larval tuna studies in the GOM. In addition, the breeding locations are similar to the areas where the bluefin bycatch by the US longline fleet is high (Block et al. 2005).

Sea surface temperature is a key oceanographic parameter for determining the location and timing of spawning in tunas, Atlantic bluefin tuna are thought to

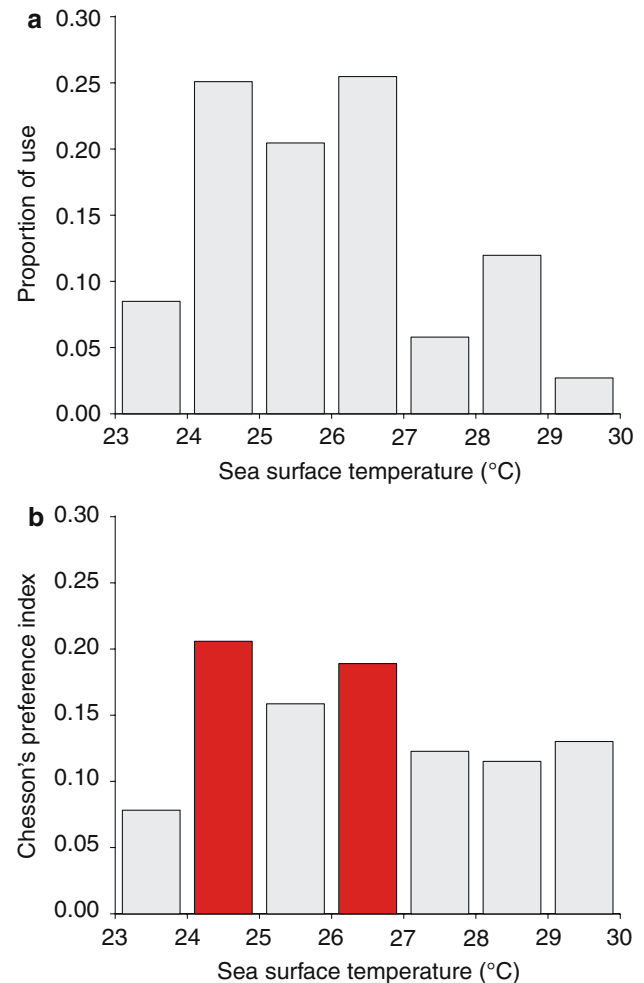


Fig. 4 *Thunnus thynnus*. **a** Observed SST habitat use of breeding phase Atlantic bluefin tuna ($n = 28$). **b** SST habitat preference of breeding phase Atlantic bluefin tuna. Red bars indicate bins where fish exhibited significant preference ($P < 0.05$, 10,000 Monte Carlo samples)

prefer SSTs in excess of 24°C for spawning (Mather et al. 1995; Block et al. 2001; Schaefer 2001; Garcia et al. 2005). Sea surface temperature was by far the most important oceanographic parameter affecting the probability of an area being used by breeding bluefin tuna because the RSF was most sensitive to SST (after longitude). The SST significantly affected the distribution of breeding phase bluefin tuna, and the fish primarily used SSTs $\geq 24^\circ\text{C}$ and preferred SSTs of 24 to 27°C. There was monthly variation in the SSTs used and preferred by the fish. For example in June, the fish primarily used areas with SSTs between 28 and 29°C but the fish do not exhibit any significant preference for these temperatures, which may indicate a lack of appropriate breeding areas with the preferred SST range during the later part of the breeding season. These high SSTs indicate that bluefin tuna occupying the GOM late in

Table 2 *Thunnus thynnus*. Monthly remotely sensed sea surface temperatures (SSTs) at locations and dates that Atlantic bluefin tuna exhibited breeding phase behavior

	April	May	June
Number of days	121	89	49
SST (°C)	24.4 ± 0.5	26.2 ± 0.5	28.6 ± 0.3

SSTs were significantly different between all months ($P < 0.001$, ANOVA)

the breeding season are likely subjected to a relatively high thermal stress. We hypothesize that high temperatures and hypoxic waters would combine to decrease survivorship for bluefin tuna caught on longlines in the GOM. It would therefore be important as a first step, to minimize the interactions between the longline fishery and the breeding bluefin tuna in the GOM during this period.

In the Balearic Archipelago, Atlantic bluefin tuna larvae were primarily found in SSTs from approximately 24 to 25°C (Garcia et al. 2005). Like most tuna species, the two other species of bluefin tuna (Pacific bluefin tuna, *T. orientalis*, and Southern bluefin tuna, *T. maccoyii*) also primarily breed in SSTs $\geq 24^\circ\text{C}$ (Bayliff 1994; Caton 1994; Schaefer 2001). In laboratory studies on Pacific bluefin tuna, the number of deformed larvae at hatching was reduced by rearing eggs at 25°C (Miyashita et al. 2000), which suggests temperature directly affects larval development. Other scombroid species also appear to prefer SSTs $\geq 24^\circ\text{C}$ for breeding. For example, swordfish off eastern Australia become more reproductively active as water temperature exceeded 24°C (Young et al. 2003).

Western Atlantic bluefin tuna in the breeding phase appeared to prefer areas with moderate eddy kinetic energy

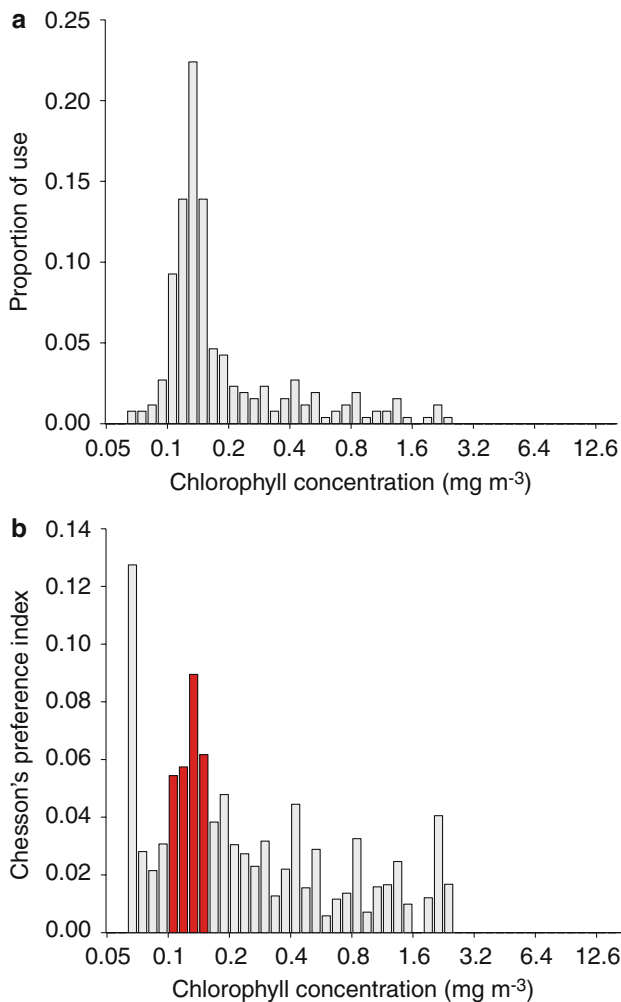


Fig. 5 *Thunnus thynnus*. **a** Observed surface chlorophyll habitat use of breeding phase Atlantic bluefin tuna ($n = 28$). **b** Surface chlorophyll preference of breeding phase Atlantic bluefin tuna. Red bars indicate bins where fish exhibited significant preference ($P < 0.05$, 10,000 Monte Carlo samples)

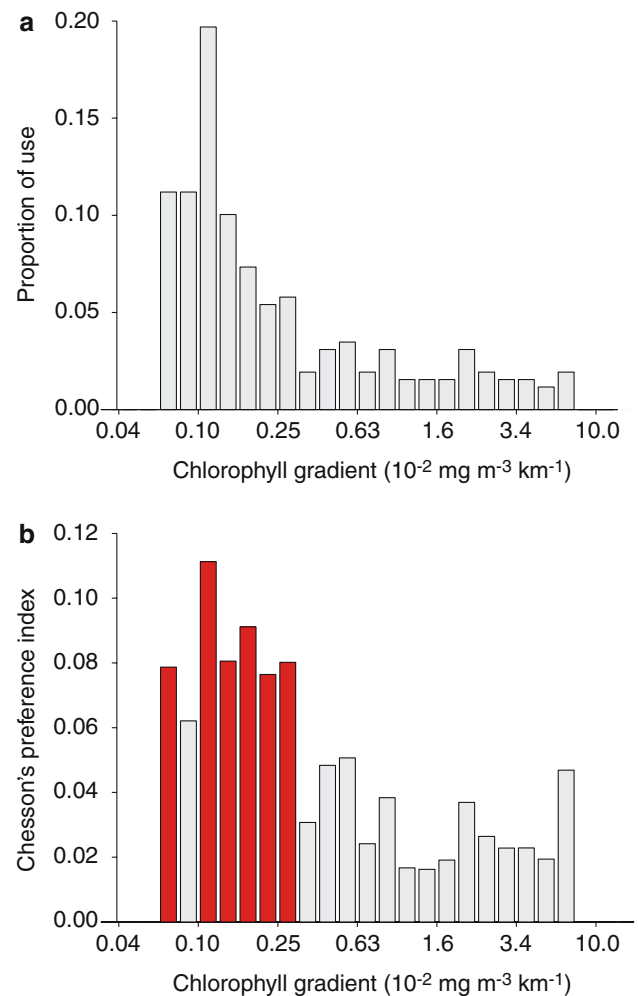


Fig. 6 *Thunnus thynnus*. **a** Observed surface chlorophyll gradient use of breeding phase Atlantic bluefin tuna ($n = 28$). **b** Surface chlorophyll gradient preference of breeding phase Atlantic bluefin tuna. Red bars indicate bins where fish exhibited significant preference ($P < 0.05$, 10,000 Monte Carlo samples)

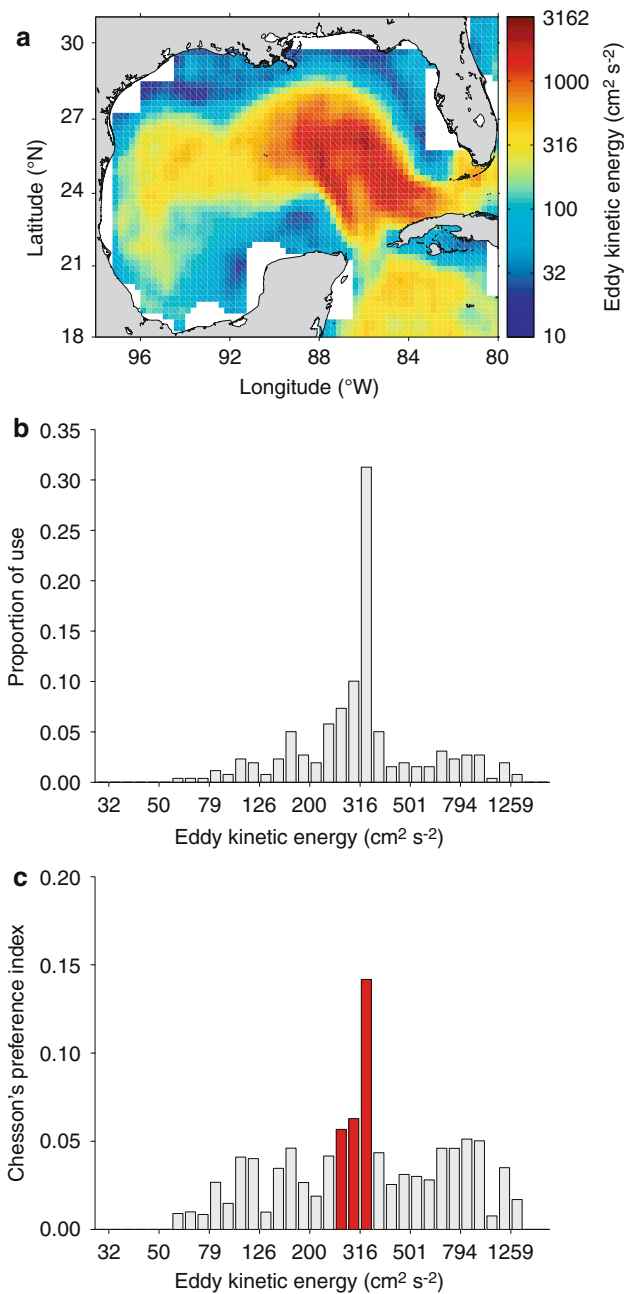


Fig. 7 *Thunnus thynnus*. **a** Eddy kinetic energy (EKE) distribution in the Gulf of Mexico. **b** Observed EKE habitat use of breeding phase Atlantic bluefin tuna ($n = 28$). **c** EKE habitat preference of fish. Red bars indicate bins where fish exhibited significant preference ($P < 0.05$, 10,000 Monte Carlo samples)

(251–355 cm² s⁻²), where mesoscale eddies are prevalent. Similarly, the discrete choice model indicated that eddy kinetic energy significantly affected the probability of breeding bluefin tuna using an area, even after taking into consideration the effects of all other parameters. Eddy kinetic energy identifies regions where phenomena like mesoscale eddies and current meanders are common (Waugh et al. 2006). The GOM has a complex environment

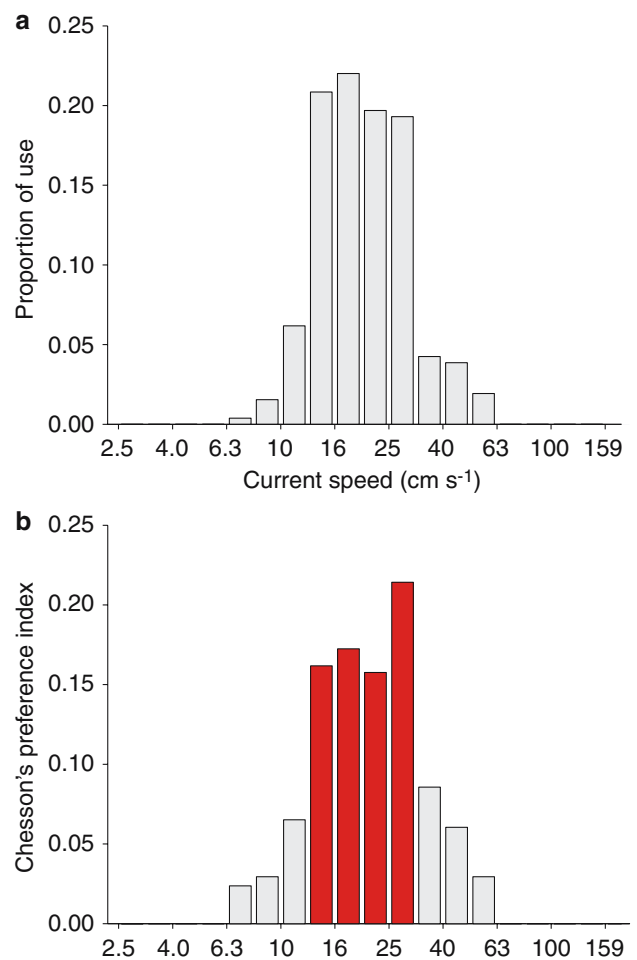


Fig. 8 *Thunnus thynnus*. **a** Observed surface current speed habitat use of breeding phase Atlantic bluefin tuna ($n = 28$). **b** Surface current speed preference of breeding phase Atlantic bluefin tuna. Red bars indicate bins where fish exhibited significant preference ($P < 0.05$, 10,000 Monte Carlo samples)

where cyclonic and anti-cyclonic eddies are generated by the Loop Current, and eddy kinetic energy measurements can be used to better define the habitat. The meanders and high current speed of the Loop Current (23 to 35 Sv, Hamilton et al. 2005) cause the eastern GOM to be an area of high eddy kinetic energy, while moderate eddy kinetic energy areas are found primarily in the western GOM.

One of the key oceanographic features in the western GOM is the cyclonic and anti-cyclonic mesoscale eddies generated by the Loop Current, which travel to the western GOM (Dietrich and Lin 1994) at speeds of 3 to 6 km day⁻¹ (Sutyryn et al. 2003). The Loop Current sheds large anti-cyclonic eddies in the eastern GOM, and these anti-cyclonic eddies in turn generate cyclonic eddies and areas with positive vorticity as they move from east to west (Dietrich and Lin 1994). The moderate eddy kinetic energy of the western GOM indicates the prevalence of these mesoscale eddies. In contrast, the shelf regions have lower

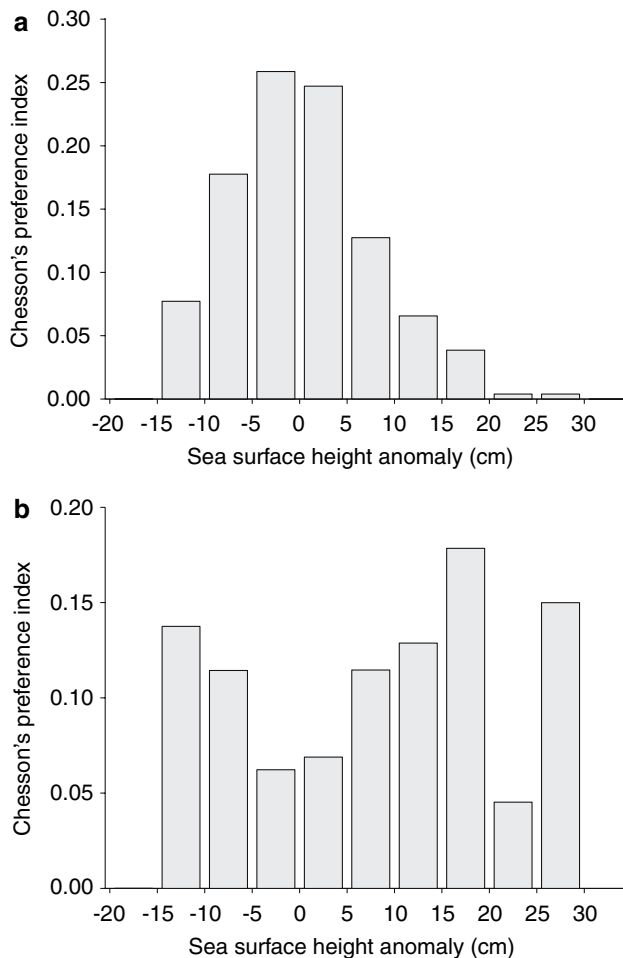


Fig. 9 *Thunnus thynnus*. **a** Observed SSHA habitat use of breeding phase Atlantic bluefin tuna ($n = 28$). **b** SSHA habitat preference of fish. Red bars indicate bins where fish exhibited significant preference ($P < 0.05$, 10000 Monte Carlo samples)

eddy kinetic energy. Cyclonic eddies and areas with positive vorticity in the GOM are associated with cooler temperatures, shallower thermoclines, and enhanced primary and secondary production (Olson 1991; Bakun 1996; Gasca 1999, 2003; Wormuth et al. 2000; Gasca et al. 2001; Suarez-Morales et al. 2002). These cooler regions may be important for adults because warm SSTs, coupled with large body sizes and increased activity during courtship and spawning, may result in increased metabolic stress. In contrast, anti-cyclonic eddies and areas with negative vorticity have enhanced retention, warmer temperatures, and deeper thermoclines (Olson 1991; Bakun 1996; Wormuth et al. 2000; Gasca et al. 2001). Bakun (1996) suggested that regions where enhanced production is followed by enhanced retention would likely improve survival and recruitment of larval fish.

Larval tuna surveys around the Balearic Archipelago in the western Mediterranean Sea have similarly suggested

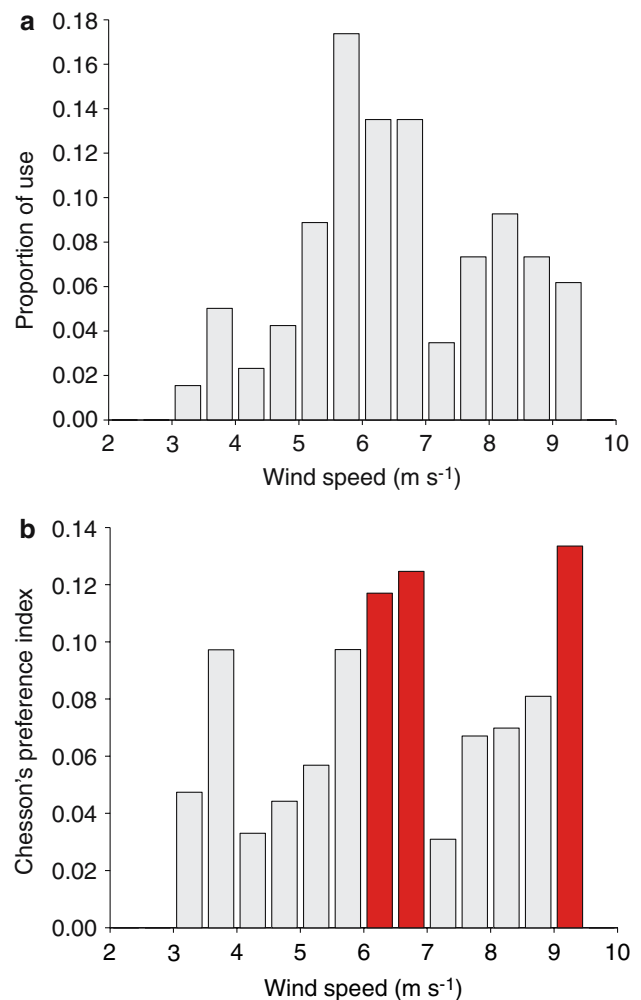


Fig. 10 *Thunnus thynnus*. **a** Observed surface wind speed habitat use of breeding phase Atlantic bluefin tuna ($n = 28$). **b** Surface wind speed preference of breeding phase Atlantic bluefin tuna. Red bars indicate bins where fish exhibited significant preference ($P < 0.05$, 10000 Monte Carlo samples)

that mesoscale eddies are likely to be important for the successful reproduction of eastern Atlantic bluefin tuna (Garcia et al. 2005). The Balearic Islands consist primarily of Ibiza, Mallorca, and Menorca in whose waters bluefin tuna are known to spawn (Platonenko and Serna 1997; Nishida et al. 1998). Based on larval tuna survey data from 2001 to 2003, Garcia et al. (2005) also suggested that bluefin tuna were spawning in mesoscale anti-cyclonic eddies south of the Balearic Islands.

The bluefin tuna exhibited some preference for areas with highly negative and/or positive SSHA but these preferences were not statistically significant. Electronic tag data are able to provide accurate, high-resolution information on the behavior and physiology of bluefin tuna, and we used this information to determine the days when the fish were likely to be breeding (Teo et al. 2007). However,

the geolocation estimates have relatively coarse spatial resolution (Teo et al. 2004). It may therefore be more difficult to determine the habitat use and preference of the breeding bluefin tuna in relation to small-scale features, such as eddies that are 50–100 km across. As the accuracy of geolocation estimates improves, our ability to analyze fish habitat use and preference in relation to these small-scale features will also improve. In comparison to SSHA, eddy kinetic energy identifies large regions where phenomena like mesoscale eddies and current meanders are important over long time scales, and is therefore less affected by geolocation error.

Our analysis showed that Atlantic bluefin tuna exhibited significant preference for the continental slope of the GOM during the breeding phase. However, the fish were most likely not directly using the continental slope of the GOM because the maximum depths exhibited by the fish during the breeding phase were relatively shallow (Teo et al. 2007). It is more likely that the fish preferred areas with mesoscale eddies, which interact with the bottom topography. As the eddies move from the eastern to the western GOM, the eddies interact with the bottom topography of the continental slope, which acts as a guide for the propagation of these eddies (Smith and O'Brien 1983; Sutyrin et al. 2003).

Surface chlorophyll concentration and gradient significantly affected habitat use of breeding phase bluefin tuna, with a significant preference for areas with low surface chlorophyll concentrations (0.10–0.16 mg m⁻³). This is similar to the surface chlorophyll concentrations for other pelagic fish species that use warm, oligotrophic waters for spawning. For example, swordfish increased their reproductive activity in waters below 0.2 mg m⁻³ (Young et al. 2003). Bluefin tuna larvae around the Balearic Islands were also found in areas with low surface chlorophyll concentrations (Garcia et al. 2005). However, they did not report the levels of surface chlorophyll associated with the bluefin tuna larvae. The low surface chlorophyll concentrations associated with bluefin tuna and other pelagic fish are likely due to their preference for spawning in warm, oligotrophic waters. This preference for warm, oligotrophic waters may reduce predation on eggs and larvae.

Wind speed is one determinant of microturbulence, which is thought to affect the feeding success and growth rate of larval fishes (MacKenzie and Leggett 1993; Dower et al. 1997). Moderate levels of microturbulence have been shown in laboratory studies to improve the feeding rate, growth, and survival of the larval stages of several species, including yellowfin and Pacific bluefin tuna (Kimura et al. 2004; Kato and Kimura 2005). Increased microturbulence increases the contact rate between larval fish and their prey; thus enhancing their feeding rate (Rothschild and Osborn 1988) but high levels of microturbulence reduce the ability

of larval fish to capture and handle prey (MacKenzie and Kiorboe 2000). In laboratory studies, Kato and Kimura (2005) showed that Pacific bluefin tuna larvae had improved feeding and survival rates at moderate levels of microturbulence with dissipation rates from approximately 3.2 to 10.0 × 10⁻⁷ m² s⁻³. Since bluefin tuna larvae are primarily in the upper 15 m of the water column, the optimal wind speed for the bluefin tuna larvae would be approximately 7.5 to 12.5 m s⁻¹ (Kato and Kimura 2005). This range appears to be slightly higher than the preferred wind speeds exhibited by the bluefin tuna in the breeding phase. This may be because using wind speed alone underestimates the level of microturbulence and prey contact rate in an area, because turbulence can also be generated from surface currents (Dower et al. 1997). In addition, the feeding rate is also dependent on the prey concentration.

When interpreting the results of the discrete choice model, it is important to note that all the parameters in the RSF should be considered at the same time. If an area has an environmental parameter that increases the probability of bluefin tuna using an area but another parameter that decreases it, the antagonistic effects of the parameters may cancel each other out. It is also important to note that it is unclear if bluefin tuna are directly cueing on specific oceanographic parameters in their breeding areas, and if so, which parameters. It is therefore useful to consider that the breeding areas used by bluefin tuna tended to have certain oceanographic characteristics rather than being specific cues.

In this study, we have quantified the habitat use and preference of Atlantic bluefin tuna on their breeding grounds in the GOM. Results of this study can be used to develop a detailed model for the breeding habitat of Atlantic bluefin tuna in the GOM and determine their essential breeding habitat. Bycatch of mature bluefin tuna in the GOM is potentially impacting the recovery of the western stock of Atlantic bluefin tuna (Block et al. 2005). If the essential breeding habitat can be identified, as we have done here, and a restricted time-area closure in the GOM developed to reduce the interaction of pelagic longlines with bluefin tuna, it may be possible to protect this important spawning habitat. Importantly, our results can form the basis of a predictive habitat-interaction model used to set up time-area closures or direct commercial fisheries to areas with lower probability of interaction. In order to minimize the impact on the fishers, the optimal time and area of closure could also be determined by comparing the habitat use and preferences of yellowfin tuna in the GOM (the target species), with bluefin tuna. The fishers could then be encouraged to fish in areas where the yellowfin catch-per-unit-effort is likely to remain high but with reduced impact on bluefin tuna. In addition, it would

be important to do a parallel study on the breeding grounds of eastern Atlantic bluefin tuna in the Mediterranean Sea and compare the results of this study. Comparative analysis will enable us to better understand how pelagic fish species use different oceanic regions during spawning, discern potential population differentiation in distinct habitats, and help delineate and protect spawning grounds of the Atlantic bluefin tuna.

Acknowledgments This study could not have been conducted without the dedication and perseverance of the Tag-A-Giant (TAG) scientific team. We thank the captains and crews of the FVs Calcutta, Bullfrog, Raptor, Tightline, Leslie Anne, 40 Something, Allison, Last Deal, and Shearwater. We thank H. Dewar, M.J.W. Stokesbury, K.C. Weng, S. Beemer, A.C. Seitz, C.J. Farwell, E.D. Prince, T. Williams, T. Sippel, G. Shillinger, and numerous others, for helping to tag bluefin tuna. The National Marine Fisheries Service assisted us greatly in tag recapture. We thank P. Gaspar for providing the surface current data. We were helped greatly by the free access to online oceanographic datasets, which were provided and maintained by NASA, NOAA, AVISO, CLS, and SIO. The manuscript was improved by helpful comments from G. Lawson, G. Somero, F. Micheli, W. Gilly, and three anonymous reviewers. Funding for this study was provided by the NOAA, NSF, Disney Conservation Fund, and the Packard, Pew, and Monterey Bay Aquarium Foundations.

References

- Arthur SM, Manly BFF, McDonald LL, Garner GW (1996) Assessing habitat selection when availability changes. *Ecology* 77:215–227
- Bakun A (1996) Patterns in the ocean: ocean processes and marine population dynamics. California Sea Grant College System, National Oceanic and Atmospheric Administration in cooperation with Centro de Investigaciones Biológicas del Noroeste, La Jolla
- Baumgartner MF, Mate BR (2005) Summer and fall habitat of North Atlantic right whales (*Eubalaena glacialis*) inferred from satellite telemetry. *Can J Fish Aquat Sci* 62:527–543
- Bayliff WH (1994) A review of the biology and fisheries for northern bluefin tuna, *Thunnus thynnus*, in the Pacific Ocean. FAO Fish Tech Pap 336/2:244–295
- Block BA, Dewar H, Farwell C, Prince ED (1998a) A new satellite technology for tracking the movements of Atlantic bluefin tuna. *Proc Natl Acad Sci USA* 95:9384–9389
- Block BA, Dewar H, Williams T, Prince ED, Farwell C, Fudge D (1998b) Archival tagging of Atlantic bluefin tuna (*Thunnus thynnus thynnus*). *Mar Technol Soc J* 32:37–46
- Block BA, Dewar H, Blackwell SB, Williams TD, Prince ED, Farwell CJ, Boustany A, Teo SLH, Seitz A, Walli A, Fudge D (2001) Migratory movements, depth preferences, and thermal biology of Atlantic bluefin tuna. *Science* 293:1310–1314
- Block B, Costa D, Boehlert G, Kochevar R (2002) Revealing pelagic habitat use: the Tagging of Pacific Pelagics program. *Oceanol Acta* 25:255–266
- Block BA, Teo SLH, Walli A, Boustany A, Stokesbury MJW, Farwell CJ, Weng KC, Dewar H, Williams TD (2005) Electronic tagging and population structure of Atlantic bluefin tuna. *Nature* 434:1121–1127
- Caton AE (1994) Review of aspects of southern bluefin tuna biology, population, and fisheries. FAO Fish Tech Pap 336/2:296–343
- Chambers RC (1997) Environmental influences on egg and propagule sizes in marine fishes. In: Chambers RC, Trippel EA (eds) Early life history and recruitment in fish population. Chapman & Hall, New York, pp 63–102
- Chesson J (1978) Measuring preference in selective predation. *Ecology* 59:211–215
- Chesson J (1983) The estimation and analysis of preference and its relationship to foraging models. *Ecology* 64:1297–1304
- Cooper AB, Millsbaugh JJ (1999) The application of discrete choice models to wildlife resource selection studies. *Ecology* 80:566–575
- Dietrich DE, Lin CA (1994) Numerical studies of eddy shedding in the Gulf of Mexico. *J Geophys Res* 99:7599–7615
- Dower JF, Miller TJ, Leggett WC (1997) The role of microscale turbulence in the feeding ecology of larval fish. *Adv Mar Biol* 31:169–220
- Ducet N, Le Traon PY, Reverdin G (2000) Global high-resolution mapping of ocean circulation from TOPEX Poseidon and ERS-1 and -2. *J Geophys Res* 105:19477–19498
- Ekstrom PA (2004) An advance in geolocation by light. In: Naito Y (ed) *Memoirs of the National Institute of Polar Research, Special Issue*. National Institute of Polar Research, Tokyo, pp 210–226
- García A, Alemany F, Velez-Belchi P, Lopez Jurado JL, Cortes D, de la Serna JM, Gonzalez Pola C, Rodriguez JM, Jansa J, Ramirez T (2005) Characterization of the bluefin tuna spawning habitat off the Balearic Archipelago in relation to key hydrographic features and associated environmental conditions. *Coll Vol Sci Pap ICCAT* 58:535–549
- Gasca R (1999) Siphonophores (Cnidaria) and summer mesoscale features in the Gulf of Mexico. *Bull Mar Sci* 65:75–89
- Gasca R (2003) Hyperiid amphipods (Crustacea: Peracarida) and spring mesoscale features in the Gulf of Mexico. *Mar Ecol Publ Stn Zool Napoli* 24:303–317
- Gasca R, Castellanos I, Biggs DC (2001) Euphausiids (Crustacea, Euphausiacea) and summer mesoscale features in the Gulf of Mexico. *Bull Mar Sci* 68:397–408
- Gaspar P, Georges JY, Fossette S, Lenoble A, Ferraroli S, Le Maho Y (2006) Marine animal behaviour: neglecting ocean currents can lead us up the wrong track. *Proc R Soc Lond Ser B* 273:2697–2702
- Hamilton P, Larsen JC, Leaman KD, Lee TN, Waddell E (2005) Transports through the Straits of Florida. *J Phys Oceanogr* 35:308–322
- ICCAT (2005) Report of the Standing Committee on Research and Statistics, 2004–2005. ICCAT, Madrid, Spain
- Johnson DH (1980) The comparison of usage and availability measurements for evaluating resource preference. *Ecology* 61:65–71
- Kato Y, Kimura S (2005) Effect of ocean turbulence on bluefin tuna, *Thunnus orientalis*, larvae. *CM 2005/O:15 ICES Annual Science Conference*. ICES, Aberdeen, UK
- Kimura S, Nakata H, Margulies D, Suter JM, Hunt SL (2004) Effect of oceanic turbulence on the survival of yellowfin tuna larvae. *Nippon Suisan Gakkai Shi* 70:175–178
- Laidre KL, Heide-Jorgensen MP (2005) Arctic sea ice trends and narwhal vulnerability. *Biol Conserv* 121:509–517
- MacKenzie BR, Leggett WC (1993) Wind-based models for estimating the dissipation rates of turbulent energy in aquatic environments: empirical comparisons. *Mar Ecol Prog Ser* 94:207–216
- MacKenzie BR, Kiorboe T (2000) Larval fish feeding and turbulence: a case for the downside. *Limnol Oceanogr* 45:1–10
- Magnuson JJ, Block BA, Deriso RB, Gold JR, Grant WS, Quinn TJ II, Sails SB, Shapiro L, Stevens ED (1994) An assessment of Atlantic bluefin tuna. National Academy Press, Washington DC
- Manly BFF, McDonald LL, Thomas DL, McDonald TL, Erickson WP (2002) Resource selection by animals: statistical design and analysis for field studies. Kluwer, Dordrecht

- Mather FJ, Mason JM Jr, Jones AC (1995) Historical document: life history and fisheries of Atlantic bluefin tuna. NOAA Technical Memorandum NMFS-SEFSC-370. NOAA, Miami
- Matthiopoulos J (2003) The use of space by animals as a function of accessibility and preference. *Ecol Modell* 159:239–268
- Matthiopoulos J, McConnell B, Duck C, Fedak M (2004) Using satellite telemetry and aerial counts to estimate space use by grey seals around the British Isles. *J Appl Ecol* 41:476–491
- McCracken ML, Manly BFJ, Vander Heyden M (1998) The use of discrete-choice models for evaluating resource selection. *J Agric Biol Environ Stat* 3:268–279
- McDonald TL, Manly BFJ, Nielson RM, Diller LV (2006) Discrete-choice modeling in wildlife studies exemplified by northern spotted owl nighttime habitat selection. *J Wildl Manage* 70:375–383
- McGowan MF, Richards WJ (1989) Bluefin tuna (*Thunnus thynnus*) larvae in the gulf stream off the Southeastern USA satellite and shipboard observations of their environment. *Fish Bull* 87:615–631
- Miyashita S, Tanaka Y, Sawada Y, Murata O, Hattori N, Takii K, Mukai Y, Kumai H (2000) Embryonic development and effects of water temperature on hatching of the bluefin tuna, *Thunnus thynnus*. *Suisanzoshoku* 48:199–207
- Nishida T, Tsuji S, Segawa K (1998) Spatial data analyses of Atlantic bluefin tuna larval surveys in the 1994 ICCAT BYP. *Coll Vol Sci Pap ICCAT* 48:107–110
- O'Brien CM, Pilling GM, Brown C (2004) Development of an estimation system for U.S. longline discard estimates of bluefin tuna. In: Payne AIL, O'Brien CM, Rogers SI (eds) *Management of shared fish stocks*. Blackwell, Oxford, pp 23–41
- Olson DB (1991) Rings in the ocean. *Annu Rev Earth Planet Sci* 19:283–311
- Pascual A, Faugere Y, Larnicol G, Le Traon P-Y (2006) Improved description of the ocean mesoscale variability by combining four satellite altimeters. *Geophys Res Lett* 33:L02611. doi:10.1029/2005GL024633
- Platonenko S, Serna JL (1997) Oceanographic and environmental observations in the western Mediterranean during the spawning season of bluefin tuna (*Thunnus thynnus* L.). *Coll Vol Sci Pap ICCAT* 46:496–501
- Polovina JJ, Balazs GH, Howell EA, Parker DM, Seki MP, Dutton PH (2004) Forage and migration habitat of loggerhead (*Caretta caretta*) and olive ridley (*Lepidochelys olivacea*) sea turtles in the central North Pacific Ocean. *Fish Oceanogr* 13:36–51
- Rice JC (2005) Understanding fish habitat ecology to achieve conservation. *J Fish Biol* 67(Suppl B):1–22
- Richards WJ, Leming T, McGowan MF, Lamkin JT, Kelley-Fraga S (1989) Distribution of fish larvae in relation to hydrographic features of the Loop Current boundary in the Gulf of Mexico. In: Blaxter JHS, Gamble JC, von Westernhagen H (eds) *The early life history of fish: the 3rd ICES Symposium*, Bergen, 3–5 October 1988. ICES, Copenhagen, Denmark
- Rothschild BJ, Osborn TR (1988) Small-scale turbulence and plankton contact rates. *J Plankton Res* 10:465–474
- Russ JC (2002) *The image processing handbook*. CRC Press, Boca Raton
- Schaefer KM (2001) Reproductive biology of tunas. In: Block BA, Stevens ED (eds) *Tunas: physiology, ecology, and evolution*. Academic Press, San Diego, pp 225–270
- Smith DI, O'Brien JJ (1983) The interaction of a two-layer isolated mesoscale eddy with bottom topography. *J Phys Oceanogr* 13:1681–1697
- Smith WHF, Sandwell DT (1997) Global sea floor topography from satellite altimetry and ship depth soundings. *Science* 277:1956–1962
- Stammer D (1998) On eddy characteristics, eddy transports, and mean flow properties. *J Phys Oceanogr* 28:727–739
- Suarez-Morales E, Gasca R, Segura-Puertas L, Biggs DC (2002) Planktonic cnidarians in a cold-core ring in the Gulf of Mexico. *Anales del Instituto de Biología Universidad Nacional Autónoma de México Serie Zoología* 73:19–36
- Sutyrin GG, Rowe GD, Rothstein LM, Ginis I (2003) Baroclinic eddy interactions with continental slopes and shelves. *J Phys Oceanogr* 33:283–291
- Teo SLH, Boustany A, Blackwell S, Walli A, Weng KC, Block BA (2004) Validation of geolocation estimates based on light level and sea surface temperature from electronic tags. *Mar Ecol Prog Ser* 283:81–98
- Teo SLH, Boustany A, Dewar H, Stokesbury MJW, Weng KC, Beemer S, Seitz AC, Farwell CJ, Prince ED, Block BA (2007) Annual migrations, diving behavior, and thermal biology of Atlantic bluefin tuna, *Thunnus thynnus*, on their Gulf of Mexico breeding grounds. *Mar Biol* 238:1–18
- Train KE (2003) *Discrete choice methods with simulation*. Cambridge University Press, New York
- Waugh DW, Abraham ER, Bowen MM (2006) Spatial variations of stirring in the surface ocean: a case study of the Tasman Sea. *J Phys Oceanogr* 36:526–542
- Wormuth JH, Ressler PH, Cady RB, Harris EJ (2000) Zooplankton and micronekton in cyclones and anticyclones in the northeast Gulf of Mexico. *Gulf Mex Sci* 18:23–34
- Young J, Drake A, Brickhill M, Farley J, Carter T (2003) Reproductive dynamics of broadbill swordfish, *Xiphias gladius*, in the domestic longline fishery off eastern Australia. *Mar Freshw Res* 54:315–332